Batteries & Supercaps

Concept
doi.org/10.1002/batt.202300503

Chemistry Europe
European Chemical Societies Publishing

www.batteries-supercaps.org

Special Collection

Na_2S Cathodes Enabling Safety Room Temperature Sodium Sulfur Batteries

Zhen Xiong,[a] Xuyuan Nie,[a] Binwei Zhang,*[a, b] and Zidong Wei*[a, b]

Room temperature sodium-sulfur (RT-Na/S) battery is regarded as a promising next-generation battery system because of their high theoretical specific capacity, and abundant availability of anodes and cathodes. Nevertheless, the direct use of sodium metal could result in the dendrite growth, causing the safety concerns. Interestingly, employing Na_2S as the cathode materials can be paired with Na-free anode to effectively avoid the problem of dendrite growth. However, the poor electronic conductivity of Na_2S and the sluggish kinetic conversion to sodium polysulfides can lead to high initial charge activation barriers and rapid capacity degradation, thereby constraining their practical application. In this concept, the electrochemical mechanism of Na_2S cathode is summarized to present the potential for RT-Na/S batteries. Additionally, recent advances on Na_2S cathodes have been discussed in detail with an emphasis on functionalized matrix, morphology modulation, and optimizing cell structure. Finally, the future opportunities and challenges for the development of Na_2S cathode based RT-Na/S batteries are proposed.

1. Introduction

Nowadays, the world is undergoing an energy revolution, and it appears increasingly probable that it will be centered around electricity.[1–4] Lithium ion batteries (LIBs) have evolved into a fundamental component of modern society, energizing a wide array of consumer electronics, including laptops, cellphones, and more.[5–7] Recently, the increasing demands for electric vehicles and energy storage systems have significantly elevated the cost of lithium salts.[8–10] Additionally, the new emerging applications usually require battery technologies characterized by low cost and high energy density. Nevertheless, the increased prices and uneven distribution of lithium resources could potentially pose risks in the supply chain.[11–15] This underscores the need to promote the development of next-generation energy storage systems beyond LIBs. On the other hand, recognizing the limited reserves of lithium, sodium has also been employed as an alternative anode since the last century.[16–19] In addition, the content of sodium in the earth's crust is 2.74 wt.%, which ranks fourth among all metals, at around $2,100 per ton ($25,000 per ton for lithium).[20–23] Therefore, it prompts the exploration and development of sodium-based battery systems that are less costly and high energy density.

Sodium sulfur (Na/S) batteries hold great potential for these new emerging energy systems thanks to their high theoretical specific capacities for both the anode and cathode (1,166 and 1,672 mAh g^{-1}, respectively), coupled with the cost-effectiveness of their cathode and anode.[24–27] In actuality, the Na-S battery initially emerged as the energy storage system more than half a century ago when the concept of the first-generation molten Na-S battery, designed to operate at a high temperature (300~350 °C), was proposed in the 1960s. Later on, it was successfully commercialized by NGK Insulator Ltd since 2003.[28–31] However, the high operating temperature above 300 °C not only increases the operating cost, but also brings certain safety risks.[32–34] Moreover, the final discharge product of high temperature Na/S battery is Na_2S_3, and thus its theoretical energy density is 760 Wh kg^{-1}.[35,36] Therefore, reducing the operating temperature is of utmost importance as it not only lowers costs but also mitigates potential safety concerns.

Recently, significant efforts have been directed towards the development of room temperature Na/S (RT-Na/S) batteries. This focus stems from the potential safety benefits associated with operating at room temperature, which can effectively mitigate the risks posed by the highly reactive molten sulfur and sodium. More importantly, RT-Na/S batteries can achieve an impressive theoretical gravimetric energy density of up to 1274 Wh kg^{-1}, owing to the complete reduction of sulfur into Na_2S.[37–39] Nevertheless, RT-Na/S batteries still face the following challenges. Firstly, Na anode would undergo the uncontrolled Na dendrite growth, and unstable solid electrolyte interphase layer (SEI) formation during discharge/charge process, resulting in low coulombic efficiency and a shorter lifespan, even short circuit.[40–42] Secondly, when S completely reduces to Na_2S, it undergoes a significant volume expansion of approximately 180%. This substantial volume expansion renders the electrode material structure highly prone to collapse, leading to a rapid

[a] Z. Xiong, X. Nie, Prof. B. Zhang, Prof. Z. Wei
School of Chemistry and Chemical Engineering
Chongqing University
Chongqing 400044 (P. R. China)
E-mail: binwei@cqu.edu.cn
zdwei@cqu.edu.cn

[b] Prof. B. Zhang, Prof. Z. Wei
Center of Advanced Electrochemical Energy
Institute of Advanced Interdisciplinary Studies
Chongqing University
Chongqing 400044 (P. R. China)

Special Collection An invited contribution to a Special Collection on Young Scientists in Battery Research.

decline in capacity.[43–47] Finally, the shuttle effect of sodium polysulfides during cycling will cause the loss of active materials, leading to a continuous decay in battery capacity.[48–52]

Na_2S, the final discharge product of RT-Na/S batteries, is considered a more favorable candidate for the initial cathode material compared to S.[53,54] It represents a fully sodiated form of sulfur, capable of being combined with sodium-free anode materials, including carbon, tin (Sn), and metal oxides. This, in turn, enhances the safety of RT-Na/S batteries.[55,56] Furthermore, this discharge product (Na_2S) is already in an expanded state, allowing to shrink during the initial desodiation process, which provides space for the volume expansion of the subsequent reaction and makes it well-suited for the fabrication of electrodes with high active substance loadings.[57,58]

While significant efforts have been invested, the development of RT-Na/S batteries with Na_2S cathodes for practical applications is still in its early stages due to the poor electronic conductivity of Na_2S and the sluggish kinetic conversion to sodium polysulfides. Here, the electrochemical mechanism and challenges of Na_2S is discussed. Furthermore, we provide a summary of strategies aimed at enhancing their electrochemical performance through the construction of functionalized matrices, adjustment of morphology, and electrode structure design. Finally, perspectives on current challenges and future directions are also proposed.

2. The Mechanism of Na_2S Cathode for RT-Na/S Batteries

The Na_2S cathode can be paired with Na-free anode materials (for example, hard carbon) to construct safe RT-Na/S batteries (Figure 1). However, when Na_2S is employed as the active material, it presents a notable energy barrier during the initial charge cycle. This is primarily attributed to the substantial phase-to-phase nuclear energy barrier that exists when converting Na_2S into sodium polysulfide, as illustrated in Figure 2a.[59]

Once the Na_2S particles have been activated following a full charge, the subsequent reaction mirrors that of sulfur as a cathode material. Figure 2b displays representative voltage profiles for the fifth cycle, offering insights into the electrochemical behavior of the Na_2S/MWCNT electrode within a half-cell configuration. The first voltage plateau registers at approximately 2.25 V, followed by a voltage slope ranging from 2.25 V to 1.65 V. This transition corresponds to the conversion of sulfur into higher-order sodium polysulfides (e.g., Na_2S_n, $4 \leq n \leq 8$). The second voltage plateau is about 1.65 V and the second voltage slope is about from 1.65 V to 1.0 V, assigned to the transition from higher-order sodium polysulfide to lower-order sodium polysulfide (e.g., Na_2S_2) or Na_2S, respectively, which are in good agreement with RT-Na/S batteries with conventional sulfur-carbon electrodes. The ex-situ UV/Vis spectroscopy and XPS also confirmed the above results. For the cathode charged to 3.2 V and discharged to 1.0 V, the band around 620 nm corresponds to S_3^-, and the broad peaks in the 400–500 nm corresponds to S_4^-, S_6^-, representing the UV/Vis characteristics of the long-chain polysulfides (Figure 2c). The S 2p spectra of

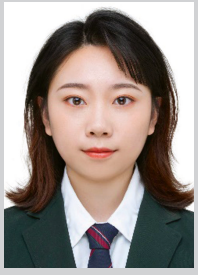

Zhen Xiong received her bachelor's degree in chemistry from the University of Jinan in 2022. She is currently working towards a master's degree at Chongqing University under the supervision of Binwei Zhang and Zidong Wei. Her research interest is room temperature sodium-sulfur batteries.

Binwei Zhang is an Associate Professor at the School of Chemistry and Chemical Engineering, and Center of Advanced Electrochemical Energy, Institute of Advanced Interdisciplinary Studies, Chongqing University. He received his bachelor's and master's degrees from Xiamen University in 2012 and 2015, respectively, and his Ph.D. degree from the Institute for Superconducting and Electronic Materials (ISEM), University of Wollongong (UOW), in 2019. He was a postdoc at the University of New South Wales and UOW. His current research interest is renewable energy storage and conversion, including electrocatalysis, lithium/sodium-sulfur batteries, and lithium/sodium-ion batteries. Homepage URL: http://hgxy.cqu.edu.cn/info/1703/5326.htm

Zidong Wei is the Chair Professor of Cheung Kong Scholars Program, Ministry of Education (China), the Chief Scientist of the National Key Research and Development Programme, and the Chief Scientist of the National Natural Science Foundation of China's major projects. He is an associate editor of Chinese Journal of Catalysis, Nano Material Science, Journal of Catalysis and Electrochemistry. His research interests are focused on catalysis, especially electrocatalysis. He has published more than 200 papers in refereed journals, and granted 27 patents associated with fuel cells. Homepage URL: http://hgxy.cqu.edu.cn/info/1519/4537.htm

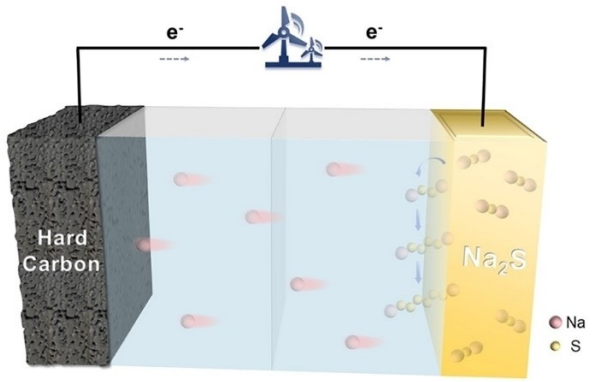

Figure 1. Schematic illustration of Na_2S cathode for RT-Na/S batteries.

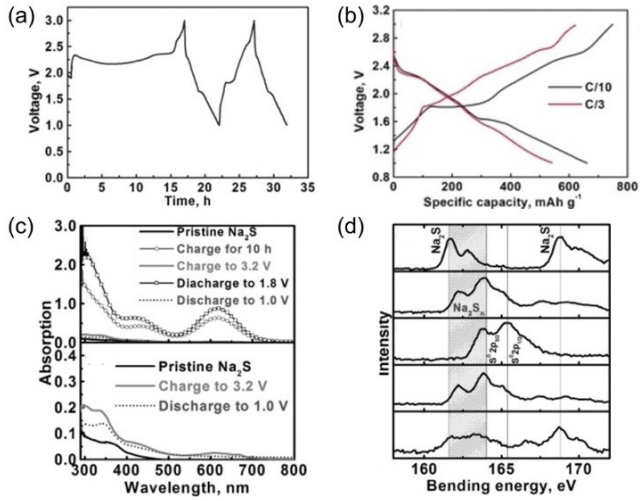

Figure 2. a) Voltage versus time profile of a RT-Na/S battery with Na_2S/MWCNT cathode. b) Voltage versus specific charge/discharge capacity profiles of the Na/Na_2S cells. c) UV/Vis absorption spectra of the pristine Na_2S/MWCNT electrode, and the electrodes charged/discharged to various states in Na/Na_2S batteries. d) High-resolution S 2p XPS spectra of Na_2S/MWCNT electrode at various states. Reproduced from Ref. [59] with permission. Copyright (2015) Wiley-VCH Verlag GmbH & Co. KGaA, Weinheim.

cathode during charging and discharging is also consistent with the characteristics of bridging sulfur atoms of the high-ordered and low-ordered polysulfides (figure 2d). The reaction during the charge and discharge cycle of Na_2S cathode cells can be expressed as:[59]

$$\text{Anode}: \ Na^+ + e^- \rightleftarrows Na \tag{1}$$

$$\text{Cathode}: \ nNa_2S \rightleftarrows Na_2S_n(4 \le n \le 8) + (2n-2)Na^+ + (2n-2)e^- \leftrightarrows nS + 2nNa^+ + 2ne^- \tag{2}$$

$$\text{Overall}: \ nNa_2S \rightleftarrows Na_2S_n(4 \le n \le 8) + (2n-2)Na \rightleftarrows nS + 2nNa \tag{3}$$

While it is possible to attain high-performance RT-Na/S batteries without using sodium anodes by employing Na_2S as the cathode, it is important to note that Na_2S exhibits low electronic conductivity. Moreover, the shuttle effect of sodium polysulfides during the charging and discharging processes also will lead to limited capacity, low Coulombic efficiency, and shorter cycle life in these RT-Na/S batteries. Moreover, the first energy barrier usually requires a high activation voltage, typically exceeding 3.5 V.[60–62] What's more, the insulating nature of Na_2S often leads to its aggregation on the electrode surface. Additionally, during the sulfur evolution reaction, the high activation energy barrier for Na_2S dissociation hinders its decomposition. Hence, achieving optimal manipulation of Na_2S necessitates the combined facilitation of robust nucleation and efficient dissociation of Na_2S. Therefore, a detailed understanding of the basic charge/discharge mechanisms of Na_2S electrodes, the design of functional bases, and the optimization of cell structures will be the focus of our future work.

3. Designing Advanced Na_2S Cathodes

The investigation of a Na_2S cathode necessitates the prior understanding of how to construct a high-performance Na_2S cathode. The preparation of such a cathode is a non-trivial endeavor due to its typically low electronic conductivity and limited reactivity. Presently, the proposed methods generally pursue two primary objectives: improving conductivity and mitigating the shuttle effect. On the basis of these recent developments, we have compiled a comprehensive overview of the strategies employed in the design of Na_2S cathodes.

3.1. Functionalized matrix

Na_2S has a low conductivity of electrons and ions (the band gap of Na_2S is 2.44 eV), so it needs to be supported on functionalized matrix with high electrical conductivity in order to enhance overall electrical performance, such as metallic materials, carbon materials, and so on.[63–66] However, metallic materials are susceptible to react with Na_2S during charging and discharging, resulting in the loss of active substances. Carbon materials exist widely in nature and has good electrical conductivity, high specific surface area and good stability; consequently, functionalized carbon-based composite materials are frequently employed as the matrix to improve the electrochemical performance of Na_2S.[67–71]

In 2015, Yu et al.[59] firstly applied Na_2S supported on multi-walled carbon nanotube (MWCNT) as cathode materials to RT-Na/S batteries. The Na_2S/MWCNT slurry was prepared by uniformly mixing Na_2S powder with short MWCNTs (5–15 mm long) and TEGDME solvent using a magnetic stirrer. The resulting slurry was then uniformly coated on the pre-treated long MWCNT (100–150 mm long) fabric electrode. Due to the advantages of MWCNT in terms of electrical conductivity, mechanical strength and specific surface area. The half-cells assembled with Na_2S/MWCNT cathode materials have a first-cycle reversible capacity as high as 660 mAh g^{-1} at a lower current density of C/10 (1C = 1675 mA g^{-1}, calculated in terms of the theoretical capacity of sulfur), whereas the first-cycle

reversible capacity decreases to 540 mAh g^{-1} when the current density is increased to C/3. After 50 cycles at current densities of C/10 and C/3, specific capacities of 560 and 380 mAh g^{-1} remained, respectively. The developed Na_2S/MWCNT electrode can easily use bulk Na_2S powder and sodium-free anode, overcoming the safety issues associated with sodium metal anodes.

Yue et al.[72] successfully reduced the size of commercial Na_2S to nanometer scale (200 nm) by using ball milling. This nanoscale Na_2S can be directly used as electrolyte and cathode material for all-solid-state Na/S batteries after sufficiently mixing with Na_3PS_4 and carbon materials. The homogeneous mixture of Na_2S, Na_3PS_4, and carbon materials ensures efficient ionic and electronic conductivity, as well as adequate interfacial contact (Figure 3a, b). By introducing nano-sized Na_2S into Na_3PS_4-C to create a Na_3PS_4-Na_2S-C nanocomposite cathode, the interfacial resistance is much lower than that of the NPS-micron-Na_2S-C composite cathode (Figure 3e), and the capacity can be increased by two times, reaching as high as 869.2 mAh g^{-1} (on the basis of Na_2S) for the first cycle at 60 °C at a current density of 50 mA g^{-1}. After 50 cycles, it can maintain a substantial capacity of 438.4 mAh g^{-1}, making it the highest reported reversible-capacity solid-state electrolyte Na/S battery at the time (Figure 3c, d). Nonetheless, the uneven distribution of Na_2S and Na_3PS_4 on the carbon material leads to a 50% decline in reversible capacity after 50 cycles.

Inspired by the casting-annealing and precipitation approach in metal production, Yue's research group employed a high-temperature casting-low-temperature annealing method to achieve a uniform incorporation of Na_2S and Na_3PS_4/C into CMK-3 mesoporous carbon (Figure 4a–c).[73] This approach establishes a stable interface between the solid electrolyte and the active materials through in situ precipitation from the outset. Consequently, it mitigates interfacial resistance between the Na_2S active nanoparticles and the Na_3PS_4 solid electrolyte. This, in turn, enhances mechanical strength, the ability to accommodate volume changes in the Na_2S active material during cycling, and overall electrochemical performance. As shown in the Figure 4d–f, at a current density of 50 mA g^{-1}, the cast-annealed Na_2S/Na_3PS_4/C composite's 60 °C all-solid-state Na/S battery has a reversible capacity of up to 800 mAh g^{-1}, which remains 650 mAh g^{-1} after 50 cycles. In sharp contrast, the reversible capacity of ball-milled Na_2S/Na_3PS_4/C cathode was 600 mAh g^{-1} for the first cycle, and rapidly decayed to 110 mAh g^{-1} after 50 cycles. The superior electrochemical performance using the low-cost raw materials with facile and sustainable synthesis of Na_2S-Na_3PS_4-CMK-3 for the low-temperature ASNSBs is an attractive approach toward promoting Na/S batteries at industrial scale.

Fujita et al.[74] prepared Na_2S-NaI solid solution as the cathode material for all-solid-state Na/S batteries by ball-milling Na_2S-NaI, vapor-grown carbon fiber (VGCF, Showa Denko) and NPS_{gc} (as a solid electrolyte) composites. After the test of ionic conductivity, the electrical conductivity increased after Na_2S-NaI mixed ball milling, and the ionic conductivity increased with the increase of NaI content, up to 2.2×10^7 S cm^{-1} (Figure 5b), which improves the conduction of sodium ions in the charging and discharging process. The initial capacity initial charging capacity was 670 mAh g^{-1} at a current density of 0.05C, which

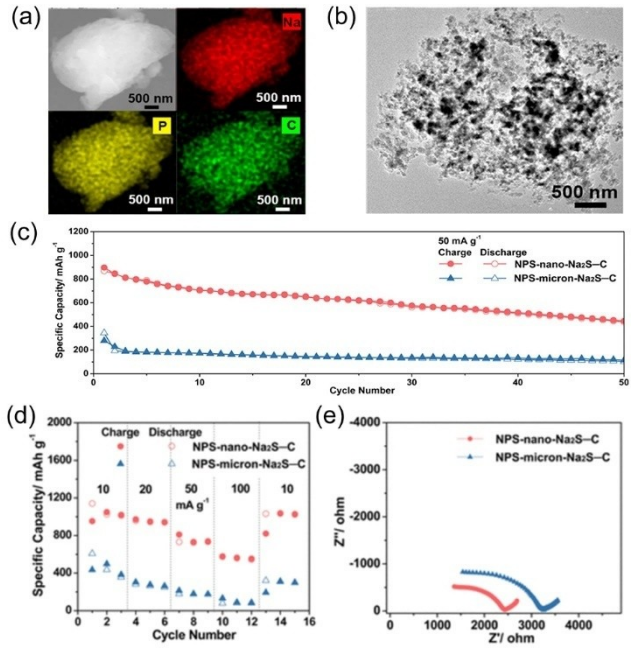

Figure 3. a) SEM image and elemental mappings of sodium, phosphorus, and carbon as well as b) TEM image for the NPS-nano-Na_2S-C nanocomposite cathode. c) Cycling performance, d) rate performance and e) EIS of NPS-micron-Na_2S-C composite and NPS-nano-Na_2S-C nanocomposite cathodes. Reproduced from Ref. [72] with permission. Copyright (2017) American Chemical Society.

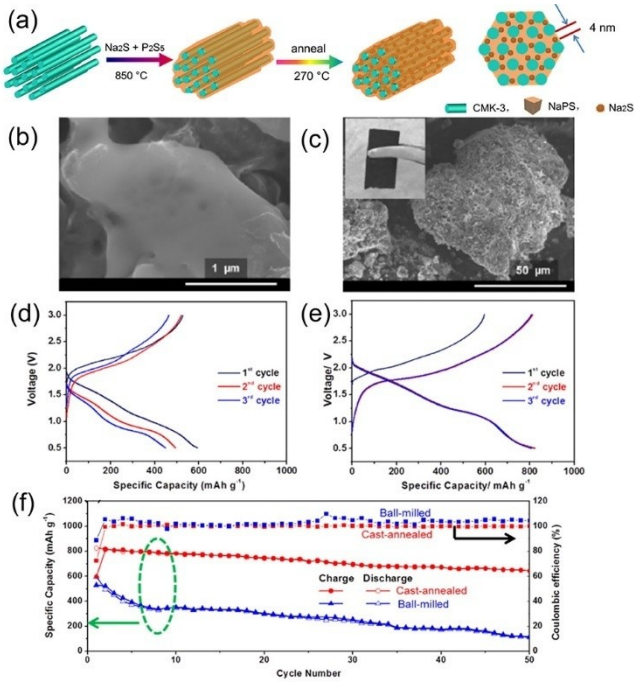

Figure 4. a) Schematic illustration of the synthesis of cast-annealed Na_2S-NPS-C composite cathode. b, c) SEM images of the annealed composite. d–f) Electrochemical performances of ball-milled Na_2S-NPS-C composite and cast-annealed Na_2SNPS-C nanocomposite cathodes. Reproduced from Ref. [73] with permission. Copyright (2018) American Chemical Society.

Concept
doi.org/10.1002/batt.202300503
Chemistry Europe
European Chemical Societies Publishing

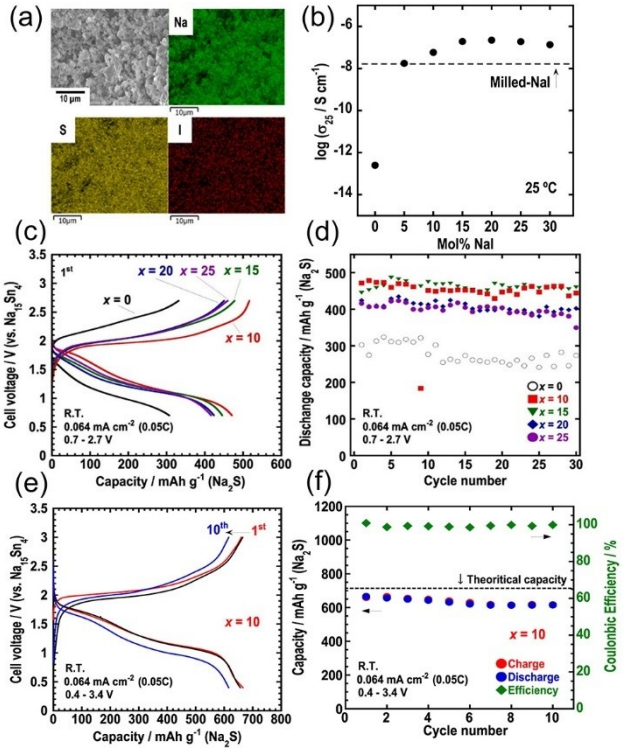

Figure 5. a) SEM-EDX images of powdered $90Na_2S{\cdot}10NaI$ sample. b) Ionic conductivities of $(100\text{-}x)Na_2S{\cdot}xNaI$($x = 0$–30 mol%) samples. c) Charge-discharge curves in 1st cycle and d) cycle performance of Na-Sn/NPSgc/$(100\text{-}x)Na_2S{\cdot}xNaI$-VGCF-NPSgc. e) Charge-discharge curves and f) cycle performance of Na-Sn/NPSgc/$90Na_2S{\cdot}10NaI$ VGCF NPSgc. Reproduced from Ref. [74] with permission. Copyright (2022) Elsevier.

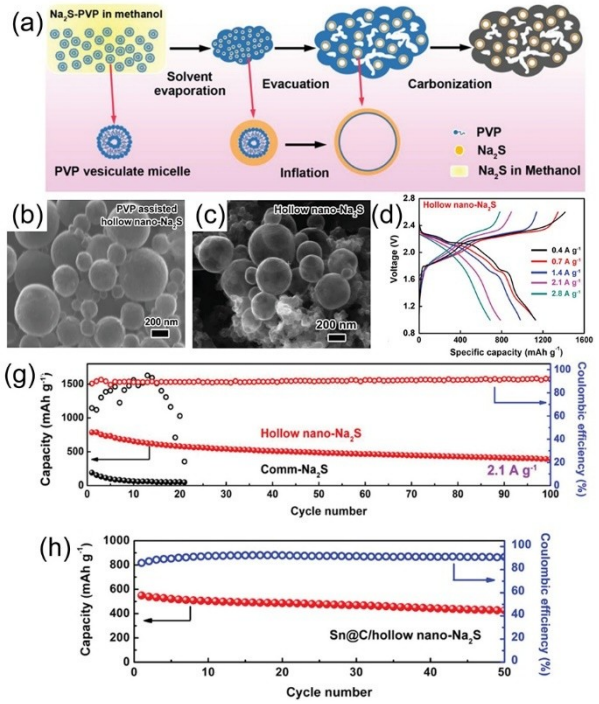

Figure 6. a) Schematic of the synthetic procedures. b) SEM images of the composite in hierarchical. c) SEM images of hollow nano-Na_2S composite cathode after ten cycles at 2.1 A g^{-1}. d, g) Half cell and h) full cell performance. Reproduced from Ref. [77] with permission. Copyright (2018) WILEY-VCH Verlag GmbH & Co. KGaA, Weinheim.

corresponds to 94% of the theoretical capacity of Na_2S. Even after 10 cycles, the discharge capacity reached 616 mAh g^{-1} with a cycling efficiency of 99.9% (Figure 5c–f).

3.2. Morphology modulation

It is well known that the morphology is play an important role in electrochemical performance; therefore, the Na_2S cathode materials performance can be tuned by systematically controlling the morphology of Na_2S.[75,76]

Hollow mesoporous carbon materials can serve as a good host structure for encapsulating Na_2S, and encapsulating Na_2S in carbon materials can effectively mitigate polysulfide solubilization. Wang et al.[77] mixed commercial Na_2S particles with polyvinylpyrrolidone (PVP) and methanol solution, and after three steps of solvent evaporation, evacuation, and carbonization, successfully prepared hollow nano-Na_2S composite (Figure 6a). The morphology of the hollow nano-Na_2S composite is similar to the structure of frog egg coral with a size of about 375 nm and a wall thickness of about 20 nm (Figure 6b, c). After ten cycles at 2.1 A g^{-1} (at the discharged state of 1 V), the morphology of the hollow nano-Na_2S composite is well maintained and could be clearly observed on the cross-section of composite cathode substrate (Figure 6d). At larger current densities of 1.4, 2.1, and 2.8 A g^{-1}, the first turn discharge capacity is as high as 980, 790, and 690 mAh g^{-1}, respectively (Figure 6e), and the Coulombic efficiency is over 90% at 2.1 A g^{-1} current density (Figure 6g). High energy density and safety are also demonstrated in Na/S full batteries paired with tin (Sn@C) sodium-free metal anode materials (Figure 6f), which have a high discharge capacity of up to 550 mAh g^{-1} on the first turn and a capacity retention rate of more than 80% after 50 turns (Figure 6h). Capacity loss due to polysulfide dissolution can also be mitigated by being virtually hermetically sealed, as the active material remains trapped in the carbon matrix and does not cause structural damage during cycling.

Moreover, the modulation of morphology via the in situ synthesis of carbon-coated Na_2S composites proves to be an effective approach. This facilitates a more intimate integration of Na_2S with electrically conductive materials, leading to a reduction in interface resistance. Thus, it can improve the conductivity of the Na_2S composite cathode and simultaneously reduce the overpotential of the first charging process.

For example, Bloi et al.[78] reported an in situ generation of Na_2S by carbothermal reduction of Na_2SO_4 with KB, a method that fulfills both the requirements of reducing the Na_2S particle size as much as possible, as well as homogeneous dispersion of Na_2S into carbon. The point is the temperature of the carbothermal reaction was selected, the Na_2S generated at different temperatures has different sizes, and the Na_2S/C-1060 composites show very porous structure (Figure 7a–c). The Na_2S/C composites synthesized at 860 °C and 960 °C reached the highest discharge capacities of 740 and 615 mAh g^{-1}. By

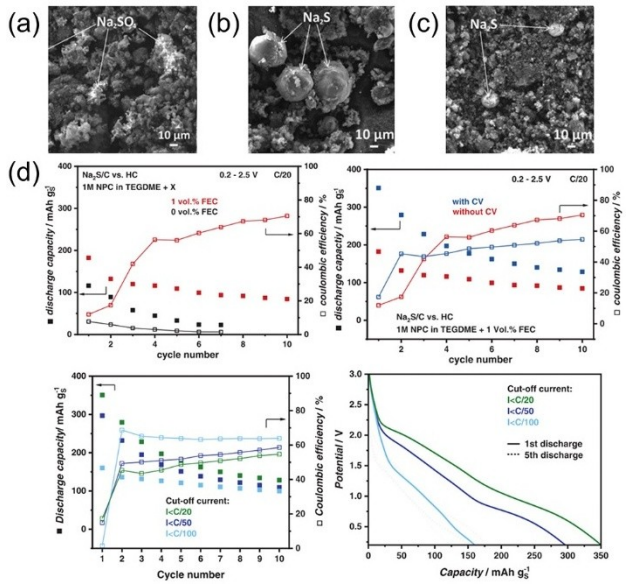

Figure 7. SEM images of the composites a) Na_2S/C-660, b) Na_2S/C-860, and c) Na_2S/C-1060, and corresponding with d) electrochemical performance of the full cells based on pristine HC and Na_2S/C-860. Reproduced from Ref. [78] with permission. Copyright (2020) WILEY-VCH Verlag GmbH & Co. KGaA, Weinheim.

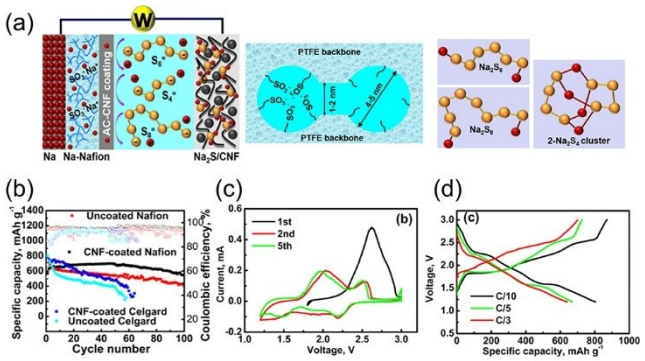

Figure 8. a) Schematic of the ionic-selectivity of the Nafion membrane by ionic interactions at the hydrophilic pores of the membrane. b) Charge-discharge profile, c) cyclic voltammograms and d) voltage versus capacity profiles of the Na//Na-Nafion/AC-CNF coating//Na_2S/AC-CNF cell. Reproduced from Ref. [87] with permission. Copyright (2016) American Chemical Society.

adding additives (1 vol% FEC) to the electrolyte and applying an excitation voltage to the first charge, the loss of active material can be reduced, thus enhancing the performance of the battery. And the longer the first charging time, the smaller the maximum discharge capacity will be, while the cycle stability of the battery will be enhanced, and the CE value will be increased (Figure 7d).

Although the Na_2S/C composites prepared by this method were able to improve the overall electrical conductivity of the anode, the obtained Na_2S size was still large (about 50 μm), resulting in a limited enhancement of the electrical conductivity of Na_2S, slower reaction kinetics, and shorter cycle life.

3.3. Optimizing electrode structure

Through the optimization and enhancement of the battery structure (separators and electrolytes) and the incorporation of functionalized electrode materials, it is expected to mitigate the detrimental impact of polysulfide shuttling. Additionally, it is possible to achieve an increased utilization of active materials and a reduction in overpotential of Na_2S.[79,80] In the subsequent section, we will delve into the optimization of electrode structure by exploring separators and electrolytes.

Separators: Separators are an important factor in batteries that prevent electrodes connection and short circuits, maintain electrolyte reservoir, and control Na^+ transport.[81,82] Therefore, researchers tried to modify the separator to block the shuttle of polysulfides.[83–86]

Yu et al.[87] designed a membrane electrode assembly with a carbon-coated Nafion membrane and a Na_2S positive electrode, which provides an avenue for the development of RT-Na/S batteries without a Na metal anode. The Nafion membrane in this membrane electrode can enhance the conduction of sodium ions, based on the estimated van der Waals size of the polysulfide, which is in the same order of magnitude as the pore size in the hydrophilic ion cluster region of the Nafion membrane. Moreover, the positively charged counterion Na^+ can migrate freely through the narrow hydrophilic pores, while the negatively charged polysulfides cannot migrate through the Nafion membrane due to the "charge repulsion" effect of the negative environment at the hydrophilic pores. According to the size effect and charge repulsion effect, the Nafion film can inhibit the shuttling of polysulfide anions. While the carbon-coated Nafion film can act as a collector, which in turn improves the electrochemical utilization of the Na_2S cathode material (Figure 8a). Compared with the conventional electrolyte-diaphragm constructed RT-Na/S battery, the Na_2S cathode material of this membrane electrode exhibits excellent RT-Na/S battery performance. The specific capacity was about 800 mAh g^{-1} at a current density of C/10, and remained at 600 mAh g^{-1} after 100 cycles (Figure 8b). The discharge capacities are about 800 mAh g^{-1}, 680 mAh g^{-1} and 640 mAh g^{-1}, respectively, at C/10, C/5, and C/3 rates (Figure 8d).

Electrolytes: Na_2S can also serve as an additive to improve the electrochemical performance of Na/S batteries. Anode SEI can be enhanced and polysulfide shuttle can be reduced by adding Na_2S complexes to the electrolyte. Kohl et al.[88] used addition of Na_2S/P_2S_5-doped tetraethylene glycol dimethyl ether electrolyte to the full cell resulted in the formation of a second SEI, which further reduced polysulfide shuttling.

Hu et al.[89] converted cost-effective Na_2SO_4 to Na_2S via a carbothermal reduction reaction, and the in situ generated Na_2S was distributed in the carbon network formed by the carbonization of polyvinylpyrrolidone (PVP). The in situ generated Na_2S is used in Na/S batteries as a desirable sodium-compensated additive with higher electrical conductivity and smaller particle size compared to commercial Na_2S, and the EDS elemental mapping results reveal the uniform distribution of C, Na, and S in Na_2S-4 (Figure 9b).

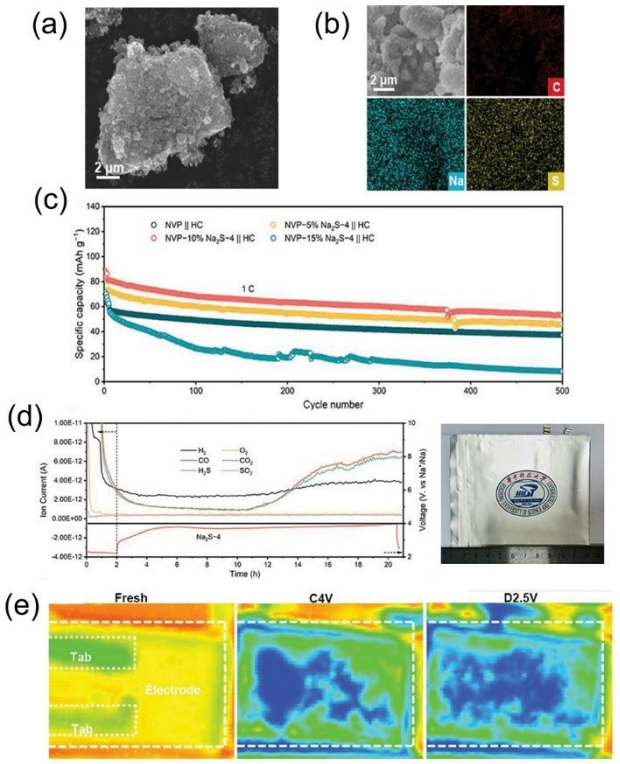

Figure 9. a) SEM image, and b) EDS elemental mappings of Na_2S-4. c) Prolonged cycle performance of full cells. d) Detection of simultaneous gas release variation curves in the in-situ DEMS tests of the Na_2S-4 half cell and the digital photograph of Na_2S-4 | |Cu pouch cell. And e) its Ultrasonic transmission mapping in three states. Reproduced from Ref. [88] with permission. Copyright (2023) Wiley-VCH GmbH.

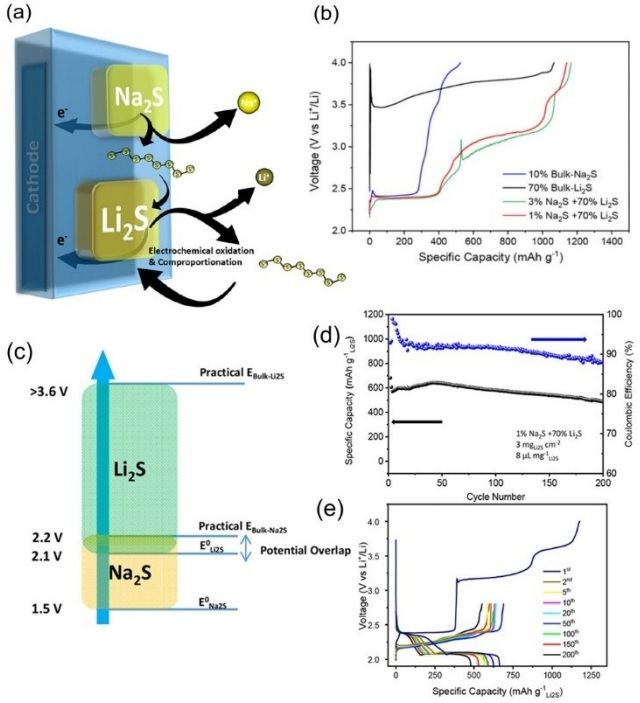

Figure 10. a) Mechanism of in situ electrochemical polysulfides injection. b) First charge profiles. c) The overlap in the practical charging voltage of Na_2S and the equilibrium Li_2S charge voltage. d–e) Cycling performance and corresponding charge/discharge voltage profiles. Reproduced from Ref. [90] with permission. Copyright (2021) American Chemical Society.

And they investigated the gas composition of the Na_2S-4 sample during the first sodium replenishment by in situ differential electrochemical mass spectrometry (DEMS). As shown in Figure 9d, the H_2, CO and CO_2 produced during the cycle, which may originate from the decomposition of the carbonate electrolyte. Moreover, they used ultrasonic scanning technique to study the integrated gas generation process within the Na_2S-4 | |Cu pouch cell (Na_2S-4 electrode material only). The blue color in Figure 9e represents a low ultrasonic transmittance, indicating the gas generation behavior. Combined with the DEMS analysis, it was observed that the gases generated in the first cycle were CO, CO_2, and H_2, which could be attributed to the decomposition of the electrolyte unrelated to the Na_2S-4 additive. This verifies the non-gas producing nature of the Na_2S-4 additive. The results showed that by doping 10 wt.% Na_2S-4 as a compensating additive into the $Na_3V_2(PO4)_3$(NVP) anode, the first discharge capacity of the full cell NVP-10% Na_2S-4 | |HC was increased by 24.3%, which corresponds to the increase in energy density from 117.2 to 138.6 Wh kg^{-1}, an increase of 18.3% (Figure 9c).

Commercial Na_2S (1-3 wt.%) was used as an in situ and localized polysulfide injector for activation of commercial Li_2S (70 wt.%) by Li et al.[90] Figure 10a illustrates the principle that Na_2S can act as a redox mediator (RM) generator in Li_2S-based cathodes, whereby polysulphides are first produced by the oxidation of Na_2S, which then facilitate the low-potential charging of Li_2S. The activation potential of Na_2S is lower than that of Li^+/Li, which was shown by LSV tests to indicate that the actual activation potential of Na_2S occurs at a voltage that overlaps well with the equilibrium potential of Li_2S. And the charging potential can be significantly reduced by adding 1–3 wt.% Na_2S into the 70% Li_2S (Figure 10b,c). After the first charge at 0.05 C, the initial discharge capacity is about 700 mAh g^{-1} (on the basis of Li_2S) at 0.1C. After 200 cycles, the capacity decayed to about 490 mAh g^{-1}(Figure 10d,e). They demonstrated that the 1 wt.% commercial Na_2S can be an in situ injector to generate polysulfides at significantly lower potentials. This in turn produces polysulfide anions around Li_2S to promote the kinetics of Li_2S activation, thereby demonstrating that employing Na_2S as a low-content electrode additive enhances the battery's capacity and cycle life.

4. Summary and Outlook

Employed the Na_2S composite material as the cathode material presents distinct advantages, including high energy density and ready availability of resources. Moreover, it circumvents the volume expansion issue typical of S-based cathodes during battery cycling. Notably, it can be coupled with Na-free anodes, thereby establishing its substantial potential as a cathode material for RT-Na/S batteries. Nevertheless, Na_2S cathode materials also face several challenges, such as low intrinsic conductivity, limited reactivity, and poor reversible cycling with

polysulfides. In addition, it also suffers from a high initial activation overpotential. Thus, it usually exists a low practical specific capacity and short cycle life. The electrochemical performance can be enhanced by compositing functionalized carbon materials with Na_2S, controlling and regulating the morphology of Na_2S, and designing the electrode structure to enhance the activation efficiency of Na_2S and improve the utilization rate of Na_2S. While considerable efforts have been made, it is crucial to remain that challenges and opportunities should be paid attention to in the future.

1) Understanding the electrochemical mechanism of Na_2S is expected to shed light on its function in RT-Na/S battery systems. A comprehensive understanding the electrochemical mechanism should be obtained, since the relationship between Na_2S structure and its electrochemical performance is unclear. Developing advanced in situ characterization techniques, such as in situ TEM, XRD, and XAS, and combining them with theoretical calculations, is essential for a more in-depth exploration of the Na_2S electrochemical mechanism during cycling.
2) Developing a simple and easily scalable method for producing Na_2S is highly desirable. Commercial Na_2S typically exhibits low capacity and a limited cycle life. Therefore, there is a pressing need for the development of a straightforward and efficient synthesis method for Na_2S. Furthermore, given Na_2S's susceptibility to moisture in ambient conditions, it is crucial to enhance its stability in the air. This can be achieved through innovative in situ synthesis methods, such as encapsulating Na_2S in specific materials. This approach is expected to improve air stability, potentially establishing a more robust connection with the surrounding atmosphere. It is anticipated that exploring new synthetic strategies that can accelerate their practical application.
3) Optimizing the cell structure holds the potential for achieving high-performance RT-Na/S batteries. Traditionally, ether-based electrolytes are used in Na_2S-based batteries, but these often encounter the shuttle effect. The introduction of diverse electrolyte additives could offer some solutions to these challenges, particularly if they are cost-effective and readily accessible. Furthermore, the incorporation of catalysts into cathode materials can expedite the conversion of polysulfides, thereby enabling high-performance RT-Na/S battery operation.

Acknowledgements

This work was supported by the National Natural Science Foundation of China (52021004, 22279011) and Fundamental Research Funds for the Central Universities (Grant No. 2023CDJXY-046).

Conflict of Interests

The authors declare no conflict of interest.

Keywords: room-temperature sodium sulfur batteries · Na_2S cathode · composites · shuttle effect

[1] S. C. L. Koh, L. Smith, J. Miah, D. Astudillo, R. M. Eufrasio, D. Gladwin, S. Brown, D. Stone, *Renewable Sustainable Energy Rev.* **2021**, *152*, 111704.
[2] K. Turcheniuk, D. Bondarev, V. Singhal, G. Yushin, *Nature* **2018**, *559*, 467–470.
[3] X. Ye, S. Luo, Z. Li, J. Ruan, Y. Pang, J. Yang, J. Wang, S. Zheng, *J. Energy Chem.* **2023**, *86*, 620.
[4] S. Koohi-Fayegh, M. A. Rosen, *J. Energy Storage* **2020**, *27*, 101047.
[5] Z. Yi, G. Chen, F. Hou, L. Wang, J. Liang, *Adv. Energy Mater.* **2021**, *11*, 2003065.
[6] G. Li, Z.-C. An, J. Yang, J.-H. Zheng, L.-F. Ji, J.-M. Zhang, J.-Y. Ye, B.-W. Zhang, Y.-X. Jiang, S.-G. Sun, *J. Mater. Chem. A.* **2023**, *11*, 14043.
[7] J. Zheng, G. Li, J. Zhang, N. Cheng, L. Ji, J. Yang, J. Zhang, B. Zhang, Y. Jiang, S. Sun, *Sci. China Chem.* **2023**, *66*, 279.
[8] M. Murugan, A. Saravanan, P. V. Elumalai, G. Murali, N. R. Dhineshbabu, P. Kumar, A. Afzal, *J. Energy Storage* **2022**, *52*, 104723.
[9] G. Zhou, H. Chen, Y. Cui, *Nat. Energy* **2022**, *7*, 312.
[10] S. Yang, X. Hu, S. Xu, A. Han, X. Zhang, N. Zhang, X. Chen, R. Tian, D. Song, Y. Yang, *ACS Appl. Mater. Interfaces* **2023**, *15*, 40633.
[11] M. Armand, J.-M. Tarascon, *Nature* **2008**, *451*, 652.
[12] D. Larcher, J.-M. Tarascon, *Nat. Chem.* **2015**, *7*, 19–29.
[13] X. Yu, A. Manthiram, *ChemElectroChem* **2014**, *1*, 1275.
[14] S. Randau, D. A. Weber, O. Koetz, R. Koerver, P. Braun, A. Weber, E. Ivers-Tiffee, T. Adermann, J. Kulisch, W. G. Zeier, F. H. Richter, J. Janek, *Nat. Energy* **2020**, *5*, 259–270.
[15] B. Zhang, Y. Jiao, D. Chao, C. Ye, Y. Wang, K. Davey, H. Liu, S. Dou, S. Qiao, *Adv. Funct. Mater.* **2019**, *29*, 1904206.
[16] Y. Qiu, J. Xu, *Nano Res.* **2023**, DOI: 10.1007/s12274-023-5993-3.
[17] C. B. Soni, V. Kumar, Z. W. Seh, *Batteries & Supercaps* **2022**, *5*, e202100207.
[18] J. A. K. Satrughna, A. Kanwade, A. Srivastava, M. K. Tiwari, S. C. Yadav, S. Teja Akula, P. M. Shirage, *Mater. Today* **2023**, DOI:10.1016/j.mattod.2023.06.013.
[19] S. Randau, D. A. Weber, O. Kötz, R. Koerver, P. Braun, A. Weber, E. Ivers-Tiffée, T. Adermann, J. Kulisch, W. G. Zeier, F. H. Richter, J. Janek, *Nat. Energy* **2020**, *5*, 259–270.
[20] M. Salama, R. Attias, R. Yemini, Y. Gofer, D. Aurbach, M. Noked, *ACS Energy Lett.* **2019** *4*, 436–446.
[21] Y. Hu, W. Wu, Z. Wen, *Energy Storage Science and Technology* **2021**, *10*, 781.
[22] Y. Wang, Y. Hao, L.-C. Xu, Z. Yang, M. Y. Di, R. Liu, X. Li, *J. Phys. Chem. C.* **2019**, *123*, 3988.
[23] Y. Liang, B. Zhang, Y. Shi, R. Jiang, H. Zhang, *Materials* **2023**, *16*, 4263.
[24] J. Zhu, L. Zeng, Y. Song, F. Peng, Y. Wang, T. He, L. Deng, P. Zhang, *J. Colloid Interface Sci.* **2023**, *647*, 546.
[25] Y. Wu, L. Wu, S. Wu, Y. Yao, Y. Feng, Y. Yu, *Small Sci.* **2021**, *1*, 2100059.
[26] Y. Wang, D. Zhou, V. Palomares, D. Shanmukaraj, B. Sun, X. Tang, C. Wang, M. Armand, T. Rojo, G. Wang, *Energy Environ. Sci.* **2020**, *13*, 3848.
[27] X. Lu, G. Xia, J. P. Lemmon, Z. Yang, *J. Power Sources* **2010**, *195*, 2431.
[28] J. L. Sudworth, *J. Power Sources* **1984**, *11*, 143.
[29] J. Zhou, S. Xu, Y. Yang, *Small* **2021**, *17*, 2100057.
[30] G. S. Li, X. C. Lu, J. Y. Kim, J. P. Lemmon, V. L. Sprenkle, *J. Mater. Chem. A.* **2013**, *1*, 14935–14942.
[31] H. Sul, A. Bhargav, A. Manthiram, *J. Mater. Chem. A* **2022**, *11*, 130.
[32] S. Zhang, Y. Yao, Y. Yu, *ACS Energy Lett.* **2021**, *6*, 529.
[33] P. Chen, C. Wang, T. Wang, *Mater. Res. Lett.* **2022**, *10*, 691.
[34] N. Tanibata, M. Deguchi, A. Hayashi, M. Tatsumisago, *Chem. Mater.* **2017**, *29*, 5232–5238.
[35] Z. Wen, J. Cao, Z. Gu, X. Xu, F. Zhang, Z. Lin, *Solid State Ionics* **2008**, *179*, 1697.
[36] H. Yang, B. Zhang, Y. Wang, K. Konstantinov, H. Liu, S. Dou, *Adv. Energy Mater.* **2020**, *10*, 2001764.
[37] J. He, A. Bhargav, L. Su, H. Charalambous, A. Manthiram, *Nat. Commun.* **2023**, *14*, 6568.
[38] X. Zhou, Z. Yu, Y. Yao, Y. Jiang, X. Rui, J. Liu, Y. Yu, *Adv. Mater.* **2022**, *34*, 2200479.
[39] E. Zhang, X. Hu, L. Meng, M. Qiu, J. Chen, Y. Liu, G. Liu, Z. Zhuang, X. Zheng, L. Zheng, Y. Wang, W. Tang, Z. Lu, J. Zhang, Z. Wen, D. Wang, Y. Li, *J. Am. Chem. Soc.* **2022**, *144*, 18995–19007.
[40] W. Liu, P. Liu, D. Mitlin, *Chem. Soc. Rev.* **2020**, *49*,7284–7300.
[41] B. Zhang, L. Ren, Y. Wang, X. Xu, Y. Du, S. Dou, *Interdisciplinary Materials* **2022**, *1*, 354.

[42] L. Ren, B. Zhang, *Exploration* **2022**, *2*, 20210182.
[43] M. Zhu, S. Li, B. Li, Y. Gong, Z. Du, S. Yang, *Sci. Adv.* **2019**, *5*, eaau6264.
[44] J. Mou, T. Liu, Y. Li, W. Zhang, M. Li, Y. Xu, J. Huang, M. Liu, J. Mater, *Chem.* **2020**, *8*, 24590–24597.
[45] F. Jin, Y. Ning, B. Wang, Z. Ren, H. Luo, Z. Zhang, N. Zhang, D. Wang, *J. Power Sources* **2023**, *565*, 232917.
[46] L. Wang, T. Wang, L. Peng, Y. Wang, M. Zhang, J. Zhou, M. Chen, J. Cao, H. Fei, X. Duan, J. Zhu, X. Duan, *Natl. Sci. Rev.* **2022**, *9*, nwab050.
[47] Z. Yan, Y. Liang, W. Hua, X.-G. Zhang, W. Lai, Z. Hu, W. Wang, J. Peng, S. Indris, Y. Wang, S. Chou, H. Liu, S. Dou, *ACS Nano.* **2020**, *14*, 10284.
[48] W. Tang, W. Zhong, Y. Wu, Y. Qi, B. Guo, D. Liu, S.-J. Bao, M. Xu, *Chem. Eng. J.* **2020**, *395*, 124978.
[49] C. Ye, H. Jin, J. Shan, Y. Jiao, H. Li, Q. Gu, K. Davey, H. Wang, S.-Z. Qiao, *Nat. Commun.* **2021**, *12*, 7195.
[50] P. Zhang, J. Wu, X. Jiang, L. Jiang, S. Lu, X. Zhao, Z. Yin, *J. Electrochem. Soc.* **2023**, *170*, 060547.
[51] C. Ye, H. Jin, J. Shan, Y. Jiao, H. Li, Q. Gu, K. Davey, H. Wang, S.-Z. Qiao, *Nat. Commun.* **2021**, *12*, 7195.
[52] B. Zhang, L. Cao, C. Tang, C. Tan, N. Cheng, W. Lai, Y. Wang, Z. Cheng, J. Dong, Y. Kong, S. Dou, S. Zhao, *Adv. Mater.* **2023**, *35*, 2206828.
[53] H. Wang, E. Matios, C. Wang, J. Luo, X. Lu, X. Hu, Y. Zhang, W. Li, *J. Mater. Chem. A* **2019**, *7*, 23747.
[54] X. Liu, Y. Tan, W. Wang, P. Wei, Z. W. Seh, Y. Sun, *ACS Appl. Mater. Interfaces* **2021**, *13*, 27057.
[55] Y.-X. Wang, B. Zhang, W. Lai, Y. Xu, S.-L. Chou, H.-K. Liu, S.-X. Dou, *Adv. Energy Mater.* **2017**, *7*, 1602829.
[56] A. K. Haridas, C. Huang, *Batteries* **2023**, *9*, 223.
[57] L. Ma, Y. Lv, J. Wu, Y. Chen, Z. Jin, *Adv. Energy Mater.* **2021**, *11*, 2100770.
[58] B. Zhang, Z. Wei, S. Sun, *Energy Storage Science and Technology* **2022**, *11*, 2811.
[59] X. Yu, A. Manthiram, *Chem. Eur. J.* **2015**, *21*, 4233.
[60] V. Kumar, A. Y. S. Eng, Y. Wang, D.-T. Nguyen, M.-F. Ng, Z. W. Seh, *Energy Storage Mater.* **2020**, *29*, 1.
[61] S. Chung, A. Manthiram, *Adv. Mater.* **2019**, *31*, 1901125.
[62] Y. Wang, J. Chai, Y. Li, Q. Li, J. Du, Z. Chen, L. Wang, B. Tang, *Dalton Trans.* **2023**, *52*, 2548.
[63] A. Kumar, A. Ghosh, A. Roy, M. R. Panda, M. Forsyth, D. R. MacFarlane, S. Mitra, *Energy Storage Mater.* **2019**, *20*, 196.
[64] N. Wang, Y. Wang, Z. Bai, Z. Fang, X. Zhang, Z. Xu, Y. Ding, X. Xu, Y. Du, S. Dou, G. Yu, *Energy Environ. Sci.* **2020**, *13*, 562.
[65] X. Peng, K. Tang, Z. Zhang, J. Hu, G. Li, J. Wang, X. Xie, N. Zhang, Z. Wu, *Nanotechnology* **2023**, *34*, 475401.
[66] S. Qian, Z. Yuan, G. Li, D. Li, J. Li, W. Han, *Chem. Eng. J.* **2023**, *471*, 144528.
[67] S.-L. Wang, J.-L. Hong, *Chem. Eng. J. Adv.* **2022**, *11*, 100352.
[68] Z. Liang, Q. Li, W. Zhang, D. Yu, W. Zhang, J. Wu, G. Wang, W. Fan, J. Wang, S. Huang, *J. Energy Chem.* **2022**, *75*, 369.
[69] Y.-M. Chen, W. Liang, S. Li, F. Zou, S. M. Bhaway, Z. Qiang, M. Gao, B. D. Vogt, Y. Zhu, *J. Mater. Chem. A* **2016**, *4*, 12471.
[70] H. Yang, Y. Lei, Q. Yang, B. Zhang, Q. Gu, Y. Wang, S. Chou, H. Liu, S. Dou, *Electrochim. Acta* **2023**, *439*, 141652.
[71] H. Yang, S. Zhou, B. Zhang, S. Chu, H. Guo, Q. Gu, H. Liu, Y. Lei, K. Konstantinov, Y. Wang, S. Chou, H. Liu, S. Dou, *Adv. Funct. Mater.* **2021**, *31*, 2102280.
[72] J. Yue, F. Han, X. Fan, X. Zhu, Z. Ma, J. Yang, C. Wang, *ACS Nano* **2017**, *11*, 4885.
[73] X. Fan, J. Yue, F. Han, J. Chen, T. Deng, X. Zhou, S. Hou, C. Wang, *ACS Nano* **2018**, *12*, 3360.
[74] Y. Fujita, A. Nasu, A. Sakuda, M. Tatsumisago, A. Hayashi, *J. Power Sources* **2022**, *532*, 231313.
[75] H. Hao, T. Hutter, B. L. Boyce, J. Watt, P. Liu, D. Mitlin, *Chem. Chem. Rev.* **2022**, *122*, 8053–8125.
[76] H. Lee, J. T. Lee, K. Eom, *Adv. Sustainable Syst.* **2018**, *2*, 1800076.
[77] C. Wang, H. Wang, X. Hu, E. Matios, J. Luo, Y. Zhang, X. Lu, W. Li, *Adv. Energy Mater.* **2019**, *9*, 1803251.
[78] L. M. Bloi, J. Pampel, S. Dörfler, H. Althues, S. Kaskel, *Adv. Energy Mater.* **2020**, *10*, 1903245.
[79] T. Yang, B. Guo, W. Du, M. K. Aslam, M. Tao, W. Zhong, Y. Chen, S. Bao, X. Zhang, M. Xu, *Adv. Sci.* **2019**, *6*, 1901557.
[80] H. Li, M. Zhao, B. Jin, Z. Wen, H. K. Liu, Q. Jiang, *Small* **2020**, *16*, 1907464.
[81] I. Bauer, S. Thieme, J. Brückner, H. Althues, S. Kaskel, *J. Power Sources* **2014**, *251*, 417.
[82] I. Bauer, M. Kohl, H. Althues, S. Kaskel, *Chem. Commun.* **2014**, *50*, 3208.
[83] X. Yu, A. Manthiram, *Matter.* **2019**, *1*, 439.
[84] C. Wang, K. Wu, J. Cui, X. Fang, J. Li, N. Zheng, *Small* **2022**, *18*, 2106983.
[85] Q. Zhao, R. Wang, J. Wen, X. Hu, Z. Li, M. Li, F. Pan, C. Xu, *Nano Energy* **2022**, *95*, 106982.
[86] J. Zeng, C. Zhao, J. Chen, F. Subhan, L. Luo, J. Yu, B. Cui, W. Xing, X. Chen, Z. Yan, *J. Chromatogr. A.* **2014**, *1365*, 29.
[87] X. Yu, A. Manthiram, *Chem. Mater.* **2016**, *28*, 896.
[88] M. Kohl, F. Borrmann, H. Althues, S. Kaskel, *Adv. Energy Mater.* **2016**, *6*, 1502185.
[89] L. Hu, J. Li, Y. Zhang, H. Zhang, M. Liao, Y. Han, Y. Huang, Z. Li, *Small* **2023**, *19*, 2304793.
[90] M. Li, J. Lu, J. Shi, S.-B. Son, D. Luo, I. Bloom, Z. Chen, K. Amine, *J. Am. Chem. Soc.* **2021**, *143*, 2185.

Manuscript received: October 27, 2023
Revised manuscript received: November 16, 2023
Accepted manuscript online: November 17, 2023
Version of record online: November 30, 2023